Received: 19 March 2017 | Revised: 22 June 2017 | Accepted: 23 June 2017

DOI: 10.1002/glia.23188

GLIA
WILEY

RESEARCH ARTICLE

KIAA1199: A novel regulator of MEK/ERK-induced Schwann cell dedifferentiation

Angélique Boerboom[1] | Céline Reusch[2] | Alexandra Pieltain[1] | Alain Chariot[2,3*] | Rachelle Franzen[1*]

[1]GIGA-Neurosciences, University of Liège, Belgium

[2]GIGA-Molecular Biology of Diseases, University of Liège, Belgium

[3]Walloon Excellence in Lifesciences and Biotechnology (WELBIO), Wavre, Belgium

Correspondence
Rachelle Franzen, GIGA Neurosciences, University of Liege, Avenue Hippocrate, 15 (quartier hopital), Bâtiment B36, +1, 4000 Liege, BELGIUM.
Email: rfranzen@ulg.ac.be

Funding information
The Belgian National Funds for Scientific Research (FRS-FNRS), the Fonds Léon Fredericq from the University of Liege, the « Fondation Charcot » from Belgium, and the « Association Belge contre les Maladies Neuro-Musculaires, ABMM »

Abstract

The molecular mechanisms that regulate Schwann cell (SC) plasticity and the role of the Nrg1/ErbB-induced MEK1/ERK1/2 signalling pathway in SC dedifferentiation or in myelination remain unclear. It is currently believed that different levels of MEK1/ERK1/2 activation define the state of SC differentiation. Thus, the identification of new regulators of MEK1/ERK1/2 signalling could help to decipher the context-specific aspects driving the effects of this pathway on SC plasticity. In this perspective, we have investigated the potential role of KIAA1199, a protein that promotes ErbB and MEK1/ERK1/2 signalling in cancer cells, in SC plasticity. We depleted KIAA1199 in the SC-derived MSC80 cell line with RNA-interference-based strategy and also generated Tamoxifen-inducible and conditional mouse models in which *KIAA1199* is inactivated through homologous recombination, using the Cre-lox technology. We show that the invalidation of KIAA1199 in SC decreases the expression of cJun and other negative regulators of myelination and elevates Krox20, driving them towards a pro-myelinating phenotype. We further show that in dedifferentiation conditions, SC invalidated for KIAA1199 exhibit lower myelin clearance as well as increased myelination capacity. Finally, the Nrg1-induced activation of the MEK/ERK/1/2 pathway is severely reduced when KIAA1199 is absent, indicating that KIAA1199 promotes Nrg1-dependent MEK1 and ERK1/2 activation in SCs. In conclusion, this work identifies KIAA1199 as a novel regulator of MEK/ERK-induced SC dedifferentiation and contributes to a better understanding of the molecular control of SC dedifferentiation.

KEYWORDS
myelin, PNS injury, differentiation, CEMIP, neuregulin

1 | INTRODUCTION

Schwann cells (SC) are the myelinating cells from the peripheral nervous system (PNS). Myelinating SCs establish 1:1 relationships with large-diameter axons and form compact myelin sheaths essential for rapid nerve conduction velocity. Non-myelinating SCs associate with small-diameter axons to form Remak bundles (Jessen & Mirsky, 2005). Besides their major roles in nerve homeostasis and myelin maintenance, SCs play key roles for repair in many pathological conditions thanks to their striking plasticity (Kim, Mindos, & Parkinson, 2013). Following injury, they are capable of reprogramming into a immature-like phenotype that drives nerve regeneration (Jessen & Mirsky, 2016). cJun, Notch or MEK1/ERK1/2 signalling belong to numerous components and signalling pathways that modulate SC dedifferentiation and peripheral nerve repair (Harrisingh et al., 2004; Woodhoo et al., 2009; Arthur-Farraj et al., 2012; Napoli et al., 2012). However, even if major progress has been made in unravelling mechanisms that regulate SC plasticity, the implication of some pathways such as Nrg1/ErbB signalling remains unclear and little is known about their temporal and quantitative activation and the interactions between them (Boerboom, Dion, Chariot, & Franzen, 2017).

KIAA1199, also known as CEll Migration Inducing Protein (CEMIP), is a 150 kDa protein whose expression is enhanced in breast, gastric, and colon cancers (Matsuzaki et al., 2009; Kuscu et al., 2012; Tiwari

*Alain Chariot and Rachelle Franzen equal contributions

et al., 2013). It was first described as an inner ear protein and genetic mutations lead to non-syndromic hearing loss (Abe, Usami, & Nakamura, 2003). The biological roles played by KIAA1199 only start to be elucidated. Indeed, KIAA1199 limits cell death, at least by promoting EGFR and other ErbB receptors stability and signalling (Shostak et al., 2014). KIAA1199 is a pro-survival protein by causing glycogen breakdown as a glycogen phosphorylase kinase β-subunit (PHKB)-binding protein (Terashima et al., 2014). KIAA1199 promotes EGF-dependent cell invasion through MEK1/ERK1/2 signalling and appears to mediate endoplasmic reticulum calcium leakage through protein kinase C alpha activation, essential for cell motility (Evensen et al., 2013). Besides, KIAA1199 also promotes hyaluronan depolymerization in skin fibroblasts (Yoshida et al., 2013). As such, KIAA1199, whose expression is elevated in the hippocampus and cerebellum, plays an important role in memory function in the central nervous system (Yoshino et al., 2017).

Since KIAA1199 promotes ErbB signalling, a key pathway for SC development and plasticity, we postulated that KIAA1199 could be necessary for these SC features. To test this hypothesis, we depleted KIAA1199 in the SC-derived MSC80 cell line with RNA-interference-based strategy and also generated inducible and conditional mouse models in which *KIAA1199* is inactivated through homologous recombination, using the Cre-lox technology. We found that if KIAA1199 is dispensable for the formation and the maintenance of the myelin in adult mice, it favors myelin breakdown after injury and maintains SC in a dedifferentiated state. Moreover, we showed that KIAA1199 deficiency in SC facilitates myelination in DRG explants and remyelination after injury, but also transiently accelerates myelination at early postnatal period. Finally, our data provide evidence that KIAA1199 is necessary for Nrg1-dependent MEK1/ERK1/2 phosphorylation. Our results identify KIAA1199 as a modulator of SC dedifferentiation, via a negative regulation of myelination, and suggest that it acts through MEK1/ERK1/2 signalling.

2 | MATERIALS AND METHODS

2.1 | Animals

The *KIAA1199* gene (Ensembl gene ID, mouse ENSMUSG00000052353) is located on chromosome 7. *KIAA1199* exon 2 harbors the translation initiation codon. The targeting vector was generated using BAC clones from the C57BL/6J RPCIB-731 BAC library (clones RP23–41L13, RP23–276P3 and RP23–1M8) and transfected into the C57BL/6N Tac ES cell line (Taconic). Exons 3 and 4 were flanked by loxP sites. Positive selection markers have been flanked by FRT (Neomycin resistance-NeoR) and F3 (Puromycin resistance-PuroR) sites and have been inserted into intron 2 and intron 4, respectively. Homologous recombinant clones were isolated using double positive (NeoR and PuroR) selection. Mutant *KIAA1199* mice were generated by Taconic. In brief, E3.5 blastocysts from superovulated BALB/c females were injected with targeted C57BL/6 ES cells and transferred to pseudopregnant NMR1 females. Chimerism was determined according to the black/white coat color, which reflects the contribution of ES cells to the BALB/c host. Highly chimeric mice were bred to C57BL/6 females and germline transmission was identified by C57BL/6 (black) in offspring by Southern blot analysis. Crossbreeding of chimeric mice with Flp Deleter mice for in vivo selection marker deletion was performed to generate mice heterozygous for the conditional KO allele. The constitutive KO allele was obtained after Cre-mediated recombination. Deletion of exons 3 and 4 results in the loss of function of KIAA1199 by generating a frameshift and a premature stop codon on exon 5. No truncated protein has been detected by western blot (WB) analysis. For genotyping analysis, the floxed allele was identified by PCR conducted on DNAs extracted from tails. Primer sequences surround each loxP site and amplify 275 bp and 455 bp products from the wild type and floxed alleles, respectively. Primer sequences are available upon request.

For inducible and conditional inactivation of *KIAA1199* in SCs (= iKO mouse), the KIAA1199$^{loxp/loxp}$ mouse was crossed with the PLP$^{CreERT/+}$ strain (B6.Cg-Tg(Plp1-cre/ERT)3Pop/J, The Jackson Laboratory) (Figure 1a). For conditional inactivation of *KIAA1199* in SCs, the KIAA1199$^{loxp/loxp}$ mouse was crossed with the Dhh$^{Cre/+}$ strain (FVB (Cg)-Tg(Dhh-cre)1Mejr/J, The Jackson Laboratory) to inactive KIAA1199 at the stage of SC precursor (embryonic day 12 of development) (= cKO mouse) (Figure 1e). *In vitro* and *ex vivo* experiments were performed on SC and dorsal root ganglions (DRG) isolated from iKO mice in the presence of 1 μM 4-OH Tamoxifen (4-OH TM) (Sigma-Aldrich) diluted in ethanol. iKO adult mice were also injected intraperitoneally twice a day during 5 consecutive days with 10 mg/mL Tamoxifen (TM) (Sigma-Aldrich) (in a mixture of sunflower oil and ethanol in proportions 9:1). Efficacy of Cre activation was assessed via YFP-immunofluorescent stainings (Figure 1d). Dhh$^{+/+}$ KIAA1199$^{loxp/loxp}$ and PLP$^{+/+}$ KIAA1199$^{loxp/loxp}$ littermates were used as controls.

2.2 | Nerve injury

Adult cKO mice were anesthetized by intraperitoneal injection of ketamine (75 mg/kg, Bayer HealthCare) and xylazine (10 mg/kg, Pfizer). Muscles of the right hind paw were carefully separated to expose sciatic nerves. For remyelination and functional recovery analysis, crushes were performed at the sciatic notch in order to allow regeneration. For myelin sheath breakdown analysis, nerves were axotomized at the sciatic notch and the proximal stump was pulled aside to favor SC dedifferentiation.

2.3 | Functional recovery tests

Sensory-motor coordination was assessed using mouse footprints to calculate the sciatic functional index. Mice were allowed to walk down a 60 cm long corridor lined with graph paper after inking their hind paws. For each animal, at least 3 footprints were obtained for each paw at every time point. The sciatic functional index was calculated as described previously (Inserra, Bloch, & Terris, 1998). Motor function was analyzed by the toe-spreading reflex (Siconolfi & Seeds, 2001). Sensory function was assessed by Von Frey Hair analysis (Vogelaar et al., 2004).

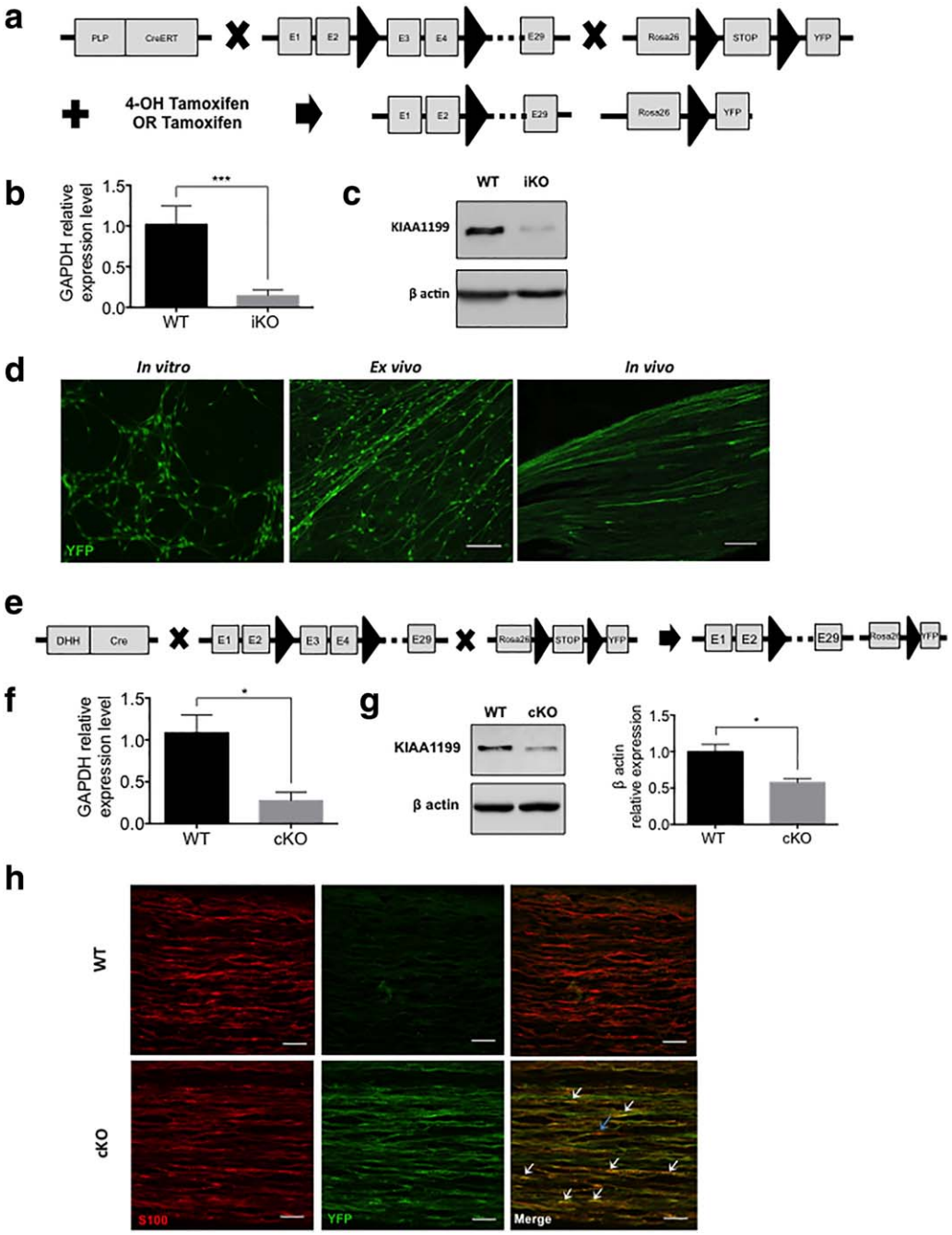

FIGURE 1 Model validation. (a) Schematic representation of the $PLP^{CreERT/+}$ $KIAA1199^{loxp/loxp}$ mouse. The KIAA1199 floxed allele is illustrated with two loxP sites (triangle) flanking exons 3 and 4. The YFP floxed allele is illustrated with two loxP sites flanking a STOP codon. The inactivation of *KIAA1199* and the expression of YFP are obtained after Cre-recombination of loxP sites induced by the addition of 4-OH TM. (b) RT-qPCR of SC primary culture extracts from $PLP^{+/+}KIAA1199^{loxp/loxp}$ (WT) and $PLP^{CreERT/+}$ $KIAA1199^{loxp/loxp}$ (iKO) mice treated for 2 days with 4-OH TM. (c) WB of primary SC protein extracts from WT and iKO mice. (d) immunofluorostaining against YFP on primary SC cultures (*in vitro*), on DRG explants (*ex vivo*) and on longitudinal sciatic nerve section (*in vivo*). (e) Schematic representation of the $DHH^{Cre/+}KIAA1199^{loxp/loxp}$ mouse. The KIAA1199 floxed allele is illustrated with two loxP sites flanking exons 3 and 4. The inactivation of *KIAA1199* is obtained after Cre-recombination. (f) Model validation. RT-qPCR analysis of SC primary culture RNA extracts from $DHH^{+/+}KIAA1199^{loxp/loxp}$ (WT) and $DHH^{Cre/+}KIAA1199^{loxp/loxp}$ (cKO). (g) WB of primary SC protein extracts from WT and cKO mice. The quantification of the WB demonstrates a decreased expression of KIAA1199. (h) immunofluorostaining against S100 (Rhodamine) and YFP (FITC) on longitudinal sciatic nerve sections from WT and cKO mice. Cre recombination is seen in a significant proportion of cKO SC (white arrows) but not in all of them (blue arrow). Statistics (b) unpaired Student's t test, $n = 3$ for WT and 5 for iKO; Scale bars (d) 100 μm (*ex vivo*) and 50 μm (*in vivo*); (h) 50 μm

2.4 | Cell culture

The mouse SC line MSC80 (a kind gift from Dr A. Baron van Evercooren, Inserm U975, Paris, France) was maintained in Dulbecco's minimal essential medium (DMEM) supplemented (Lonza) with 10% fetal bovine serum (FBS) (ThermoScientific), 100 U/mL penicillin, 100/mL streptomycin (ThermoScientific), and 0.5 g/mL fungizone (ThermoScientific).

Adult SCs were isolated from sciatic and trigeminal nerves of $PLP^{CreERT/+}$ $KIAA1199^{loxp/loxp}$ or $PLP^{+/+}$ $KIAA1199^{loxp/loxp}$ mice, as described previously (Chaballe et al., 2011). After careful dissection, nerves were left for 2 weeks in pro-degeneration medium: DMEM, 10% FBS, fungizone (2.5 mg/mL, ThermoScientific), forskolin (2 mM, Calbiochem), gentamycine (ThermoScientific) and Heregulin-β1 (Nrg1) (10 ng/mL, R&D Systems) at 37°C, 5% CO_2. After enzymatic (3 h in 0.3 mg/mL collagenase I and 2.5 mg/mL dispase II in Leibovitz medium) and mechanical dissociations, cells were plated on pre-coated poly-L-lysine (50 μg/mL, Sigma-Aldrich) and laminin (20 μg/mL, Sigma-Aldrich) culture dishes and incubated at 37°C, 5% CO_2 in $N2^{HRG}$ medium: 50% DMEM 50% F12 supplemented with N2 (ThermoScientific), gentamycin (50 μg/mL), fungizone (2.5 μg/mL), forskolin (2 μM), and Nrg1 (10 ng/mL). A few days before confluence, inactivation of *KIAA1199* was induced by the addition of 1 μM 4-OH TM (Sigma-Aldrich) for 2 days in the medium of all cultures.

2.5 | Lentiviral infections

The control or shRNAs targeting KIAA1199 were purchased from Sigma-Aldrich. Lentiviral infections in MSC80 cells were performed as previously described (Creppe et al., 2009). Briefly, 293FT cells (3×10^6) were transfected with 12 mg of the "non-target" lentiviral shRNA plasmid (used as negative control) or with the shRNA construct that targets KIAA1199, 12 mg of R8.91 and 5 mg of VSVG plasmid, using the Mirus Bio'sTransIT-LT1 reagent. The supernatants of those infected cells were filtered (0.2 mm) 48 h after transfection and added with polybrene (8 mg/mL) to 4×10^5 MSC80 cells. This latter step was repeated one more time after 24 h.

2.6 | SC dedifferentiation

In order to study SC dedifferentiation *in vitro*, sciatic and trigeminal nerves were harvested from P9 $PLP^{CreERT/+}$ $KIAA1199^{loxp/loxp}$ and $PLP^{+/+}$ $KIAA1199^{loxp/loxp}$ mice used as control. After enzymatic (3 h in 0.3 mg/mL collagenase I and 2.5 mg/mL dispase II in Leibovitz medium) and mechanical dissociations, cells were plated on pre-coated poly-L-lysine (50 μg/mL) and laminin (20 μg/mL) glass coverslips in 24-well plates. The medium consisted of DMEM supplemented with 3% FBS, forskolin (2 mM), gentamycine (50 mg/mL) and Nrg1 (10 ng/mL) and was replaced at 70% every 2 days. For *KIAA1199* inactivation, all cultures were treated with 1 μM 4-OH TM for the first 2 days. 1, 3, 5, 7, and 10 days after plating, SCs were fixed with 4% paraformaldehyde for 15 min and processed for immunocytochemistry.

In order to study SC dedifferentiation *ex vivo*, sciatic (tibial) nerves were harvested from P9 $PLP^{CreERT/+}$ $KIAA1199^{loxp/loxp}$ and $PLP^{+/+}$ $KIAA1199^{loxp/loxp}$ mice, cut in 5 mm segments and left for 4 days in pro-degeneration medium. 1 μM 4-OH TM was added to the medium for the first 2 days. Sciatic nerves were then harvested and processed for electron microscopy (EM).

2.7 | Ex vivo DRG myelination culture

DRGs from E13.5 $PLP^{CreERT/+}$ $KIAA1199^{loxp/loxp}$ or $PLP^{+/+}$ $KIAA1199^{loxp/loxp}$ mice were plated on Matrigel (BD Biosciences)-coated chamber slides in Neurobasal medium (1–2 DRG per well). After 1 week in Neurobasal medium supplemented with 2 mM Glutamine, 100 U/mL penicillin, 100 U/mL streptomycin, B27 supplement (ThermoFisher), 50 ng/mL NGF (Merck Millipore), SCs were aligned along the axons. For *KIAA1199* inactivation, cultures were treated with 1 μM 4-OH TM for 2 days in the Neurobasal medium just before switching to myelination medium (DMEM, N2 supplement, 50 ng/mL NGF, 2.5% horse serum (ThermoScientific), 20 μg/mL BPE (ThermoFisher), 0.5 μM forskolin, 100 U/mL penicillin, 100 U/mL streptomycin) supplemented with 50 μg/mL of freshly dissolved ascorbic acid (Sigma-Aldrich) to induce basal lamina formation and myelination. After 2 weeks of replacing 70% of the medium every 2 days, cultures were fixed with 4% paraformaldehyde and processed for immunochemistry (He et al., 2010). The number of MBP-positive segments/field was quantified (3–5 fields/well, 4–6 wells/embryo, 9–12 embryos out of 3 independent cultures).

2.8 | Electron microscopy

Mice were perfused with a solution containing 2.5% glutaraldehyde in 0.1 M cacodylate buffer pH 7.2. Sciatic nerves were harvested and postfixed with this solution for 2 h at 4°C, washed twice in 0.1 M cacodylate buffer, and postfixed with 1% osmium in PO_4 buffer for 30 min at 4°C. Sciatic nerves were progressively dehydrated in successive ethanol baths and then soaked in epoxypropane twice during 10 min. Tissues were embedded in epon resin by soaking in a mixture of epoxypropane/epon in proportions 2:1, then 1:1 and finally 1:2, for 1, 2, and 3 h, respectively. Sciatic nerves were then soaked in epon resin overnight before hardening the resin at 60°C for 2 days. The blocks were trimmed, and semi-thin (1 μm) and ultra-thin (75 nm) cross-sections were cut with a microtome. Semi-thin sections were collected onto glass slides, and dried on a hot plate before staining with 0.5% toluidine blue. Ultra-thin sections were contrasted with 5% uranyle-acetate and lead citrate. Four to five photographs of semi-thin sections of tibial nerve 3 mm from the sciatic notch were taken at 40×. Intact myelin sheaths were manually counted within non-overlapping successive fields covering the entire nerve section, and results were expressed as mean ± standard errors of mean of intact myelin sheaths per 1000 μm^2 of nerve tissue. For myelin sheath thickness measurements, 20 photographs of ultrathin sections of tibial nerve 3 mm from the sciatic notch were taken at 2500×. The *g* ratio was calculated for each myelinated fiber (axon diameter divided by diameter of the axon and myelin sheath).

TABLE 1 List of primers used in qPCR experiments

Gene	Forward	Reverse
Krox20	CAGGAGTGACGAAAGGAA	ACCAGAGGCTGAAGACTG
cJun	TTGAAAGCGCAAAACTCC	CTGCTGCGTTAGCATGAGTT
Notch1	ACAGTGCAACCCCCTGTATG	TCTAGGCCATCCCACTCACA
GDNF	CTGAAGACCACTCCCTCG	GACGTCATCAAACTGGTC
BDNF	TGCATCTGTTGGGGAGAC	GCCTTCATGCAACCGAAG
DDIT4	GGGATCGTTTCTCGTCCTCC	TGAGGAGTCTTCCTCCGGC
Egr1	CACCTGACCACAGAGTCCTTT	GGGAGAAGCGGCCAGTATAG
Egr3	AGATCGGGAAGGCTTGGTTG	CACATTCTCTCCCTCCAGTCG
Hbegf	AAGGACTACTGCATCCACGG	GGAGGCATTTGCAAGAGGGA
Fermt2	AGAGCAAACAGATAACAGCACG	CAGAGACTGCCAGGCTTGAA
Fosb	CGACTTCAGGCGGAAACTGA	TTCGTAGGGGATCTTGCAGC
Sik1	GGCTTTTACGACGTGGAACG	ATTGCAACCTGCGTTTTGGT
Hes1	CACCGGACAAACCAAAGACG	GGAATGCCGGGAGCTATCTT

2.9 | Immunostaining

The immunostainings on MSC80 cells, primary cells and DRGs explants were performed as followed: Nonspecific binding was prevented by 1 h incubation in a 5% donkey serum solution in 0.25% triton-PBS (0.1 M, pH 7.4). After overnight incubation at room temperature with the specific primary antibodies, sections were rinsed with PBS and incubated for 2 h at room temperature with their respective secondary antibodies coupled to Rhodamine or FITC (1:500, Jackson ImmunoResearch or Invitrogen). They were then rinsed in PBS and distilled water, dried and mounted with Safemount. Mouse anti-cJun antibody was obtained from BD Transduction Laboratories (1:500), chicken anti-GFP antibody from Abcam (1:500), rabbit anti-S100 from DakoCytomation (1:500), rat anti-MBP from Chemicon (1:250), rabbit anti- β III tubulin from Eurogentec (1:1000).

2.10 | Western blotting

Cells or sciatic nerves were lysed with RIPA buffer (10 mM Tris-HCl, pH 7.5, 150 mM NaCl, 0.1% SDS, 1% NP40, 0.1% sodium deoxycholate, 1 mM EDTA, 1 mM NaF, 10 mM Na_3VO_4, and proteases inhibitors). Cellular extracts were cleared by centrifugation (10,000g) for 10 min at 4°C and 5–50 μg of proteins were separated by SDS-PAGE and transferred to 0.45 μm nitrocellulose membranes (GE Healthcare). Membranes were blocked for 1 h in 5% non-fat milk PBS- 0.1% Tween 20 and incubated overnight at 4°C with specific primary antibodies followed by incubation with HRP-conjugated secondary antibodies for 2 h at room temperature (HRP-conjugated anti-mouse, anti-rabbit 1:10,000, GE Healthcare). Membranes were developed using ECL reagent (Thermo Scientific). The following antibodies were used: homemade rabbit anti-KIAA1199 (1:500), mouse anti-cJun (1:500, BD Transduction Laboratories), rabbit anti-ErbB3 (1:1000, Cell Signalling), rabbit anti-phospho MEK1 and anti-MEK1 (1:1000, Cell Signalling), rabbit anti-phospho ERK1/2 and anti-ERK1/2 (1:1000, Cell Signalling), mouse anti-β tubulin (1:1000, Abcam) and HRP-conjugated anti-β actin (1:10 000, Sigma-Aldrich).

2.11 | RNA extraction and real-time PCR

Total RNAs from MSC80 cells and primary SCs were extracted using the Rneasy Mini kit (Qiagen) according to manufacturer's instructions. cDNAs were synthesized using the Revert Aid H Minus First Strand cDNA Synthesis kit (Fermentas). Subsequent PCRs were performed using the Power SYBR Green PCR Master kit (Takara Bio Inc.) on the LightCycler 480 (Roche). The mRNA level was expressed relative to the mean of all control samples and normalized with glyceraldehyde-3-phosphate dehydrogenase (GAPDH) (Table 1).

2.12 | RNA sequencing

Total RNAs from MSC80 cells (control or KIAA1199 depleted, $n = 5$) were extracted using the RNeasy Mini kit (Qiagen) according to the manufacturer's protocol. Library preparation and sequencing were performed at the GIGA Genomics facility (University of Liège, Belgium). RNA integrity was verified on the Bioanalyser 2100 with RNA 6000 Nano chips, and RIN scores were >9 for all samples. The Illumina TruSeq® Stranded mRNA was used to prepare libraries from 500 ng total RNAs. PolyA RNAs were purified with polyT-coated magnetic beads, chemically fragmented, and used as template for cDNA synthesis using random hexamers. cDNA ends were subsequently end-blunted, adenylated at 3′OH extremities, and ligated to indexed adaptors. Finally, the adapters ligated library fragments were enriched by PCR following Illumina's protocol and purified with Ampure XP magnetic beads. Libraries were validated on the Bioanalyser DNA 1000 chip and quantified by

qPCR using the KAPA library quantification kit. Sequencing was performed on NextSeq500 in 75 base pair reads. For data analysis, Fastq files were trimmed using bcl2fastq2 Conversion Software. The reads were aligned with Tophat 2.0.9. Cufflinks 2.1.1 suite was used to normalize data and generate FPKM values and CuffDiff 2.1.1 was used to identify significantly differentially expressed genes. Generated lists were used to run GSEA in order to match gene sets curated from the literature.

2.13 | Statistical analysis

Data are plotted as mean values ± standard errors of mean (SEM). Statistics for dual comparisons were generated using unpaired Student's *t*-tests, and statistics for multiple comparisons were generated using one-way ANOVA or two-way ANOVA followed by Dunnet's and Sidak's post hoc tests (GraphPad Prism software); *: $p < 0.05$, **: $p < 0.01$, ***: $p < 0.001$ for all statistics herein.

3 | RESULTS

3.1 | Model validation

To investigate the role of KIAA1199 in SCs, we generated a mouse model in which exons 3 and 4 of the *KIAA1199* gene were flanked with LoxP sites ($KIAA1199^{loxp/loxp}$) (Supporting Information, Figure S1a). The deletion of the exons 3 and 4 mediated by a Cre recombinase results in a frameshift leading to a premature Stop codon and the loss of function of KIAA1199. In order to obtain an inducible knockout model (iKO), we crossed our KIAA1199 floxed strain with transgenic mice having a Tamoxifen inducible Cre-mediated recombination driven by the proteolipid protein promoter ($PLP^{CreERT/+}$) (Figure 1a). We validated the 4-OH TM-induced Cre-recombination by demonstrating a significant reduction of KIAA1199 mRNA (using exon 3-specific primers) and protein levels in SC primary culture extracts (Figure 1b and c). As we additionally crossed our conditional knockout mouse with a mutant strain having a floxed-STOP sequence followed by the *Yellow Fluorescent Protein* (YFP) gene, we also showed Cre activation via the expression of YFP by performing immunohistochemistry analysis on primary cultured SC, DRG explants and sciatic nerve sections (Figure 1d).

We also crossed the KIAA1199 floxed mouse with another transgenic mouse in which the Cre recombinase expression is under the control of the desert hedgehog (DHH) promoter (= cKO mouse) (Figure 1e). The Cre-driven recombination efficiency was demonstrated in primary SC cultures in both real-time PCR and WB analyses (Figure 1f and g, respectively). Even though KIAA1199 protein expression is decreased in the cKO primary SCs compared to WT, it should be pointed out that the protein is still present at about 50% (Figure 1g). When we assessed the Cre recombination by immunostaining against YFP on sciatic nerve sections from adult mice, it appeared that not all SCs express the YFP, demonstrating that the recombination is not 100% effective (Figure 1h).

3.2 | KIAA1199 is required to maintain pro-dedifferentiation or pro-regeneration markers in MSC80 cell line and in primary SC

Using two different short hairpin RNA (shRNA) lentiviral constructs to deplete KIAA1199 in the MSC80 SC-derived cell line, we revealed a shift of the transcriptional expression program from dedifferentiated toward differentiating SCs. Indeed, real-time PCR analysis demonstrated an increased expression of the pro-myelinating transcription factor Krox20 and a decreased expression of multiple pro-dedifferentiation factors such as cJun, Notch1, DDIT4, Egr1, and Egr3 but also of pro-regeneration factors (expressed in dedifferentiated SCs after injury) like GDNF and BDNF (Figure 2a). We also showed a reduced cJun protein expression in KIAA1199-depleted MSC80 cells through WB and immunocytochemistry analyses (Figure 2b and c, respectively).

Same results were obtained with extracts from primary SCs from iKO mice, confirming the shift of the transcriptional expression program from dedifferentiated toward differentiating SCs (Figure 2d). RT-qPCR analyses, as well as WB and immunocytochemistry against cJun reveal similar results of a reduced dedifferentiation phenotype when *KIAA1199* is inactivated in primary SCs (Figure 2d-f).

3.3 | KIAA1199 is necessary for SC dedifferentiation

To further evaluate the role of KIAA1199 in SC dedifferentiation, we took advantage of our inducible and conditional knockout mouse model (iKO) to perform *in vitro* and *ex vivo* assays to assess myelin breakdown. First, we cultured myelinating SCs isolated from postnatal day 9 (P9) WT and $PLP^{CreERT/+}$ $KIAA1199^{loxp/loxp}$ nerves (Cre-recombination assessed via anti-YFP immunostaining as illustrated on Figure 3a) and analyzed the disappearance of myelin basic protein (MBP) by double immunofluorescent cytochemistry against S100 and MBP (as illustrated on Figure 3b) over a 10 days period of time. We showed that KIAA1199-invalidated cultures contain significantly more MBP positive SCs after 10 days compared to WT cultures, respectively 81.20% ± 4.50 and 46.22% ± 10.60 (Figure 3c). This tendency was supported by EM analysis of the myelin sheath fragmentation of nerve explants after 4 days in pro-degeneration medium. The number of intact myelin sheaths was higher in $PLP^{CreERT/+}$ $KIAA1199^{loxp/loxp}$ nerves (12.10 ± 0.81) compared to WT (9.61 ± 0.81) (Figure 3d and e). Therefore, myelin clearance is significantly less effective when *KIAA1199* is inactivated.

Because KIAA1199 deficiency in SCs was shown to promote a shift of the transcriptional expression program toward differentiating SCs, we investigated whether the myelination process could be influenced by pro-myelinating signals. To address this issue, we cultured DRG explants from E13.5 $PLP^{CreERT/+}$ $KIAA1199^{loxp/loxp}$ and WT mice and let the dedifferentiated SCs migrate along the growing neurites before adding 4-OH TM to inactivate *KIAA1199*. We then induced myelination with fresh ascorbic acid-containing medium. After two weeks, the co-cultures were fixed and processed for double anti-MBP and anti-βIII tubulin immunofluorescent stainings (Figure 3f). We

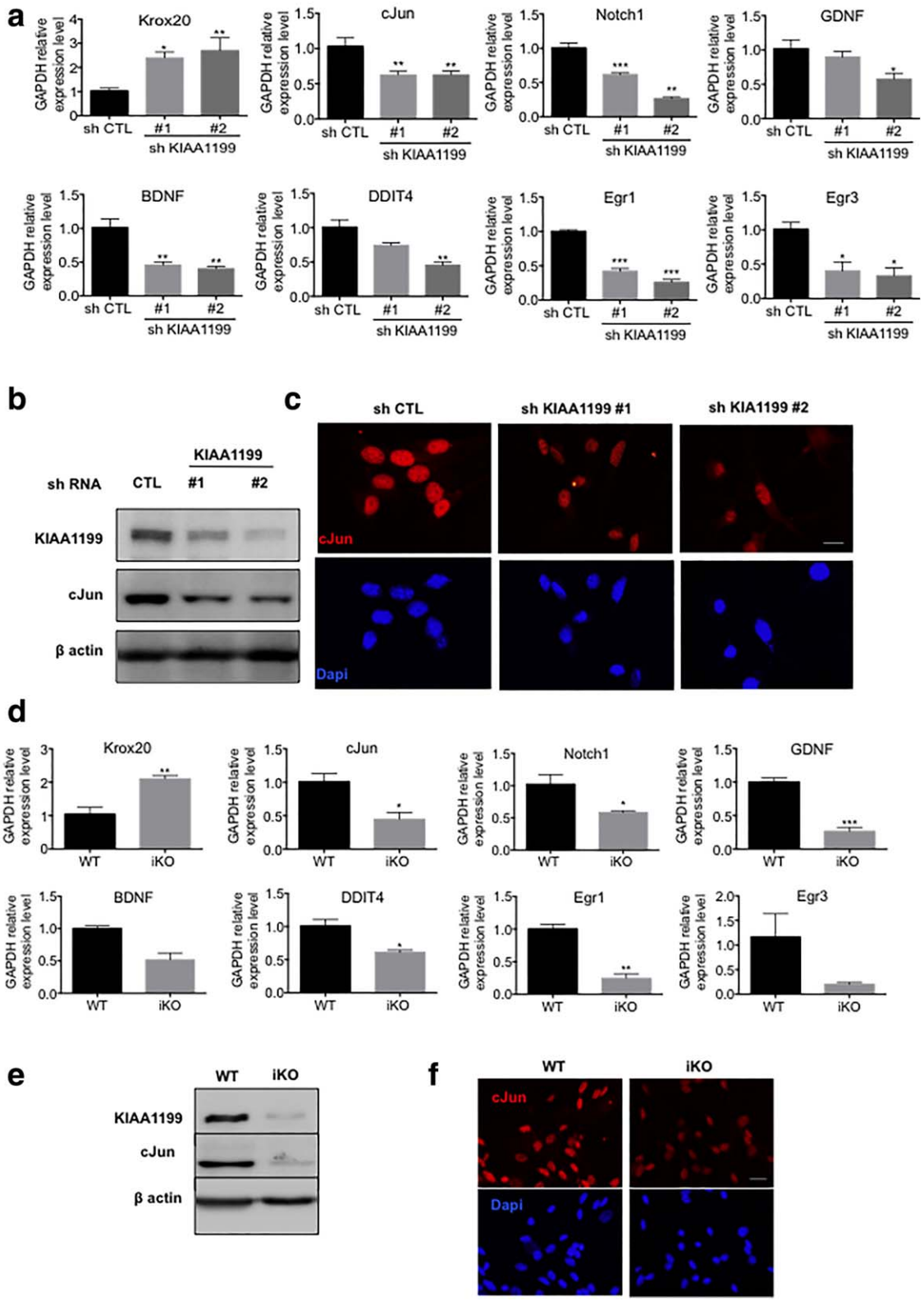

FIGURE 2 KIAA1199 deficiency decreases SC dedifferentiation and regeneration markers. (a) RT-qPCR and (b) WB of MSC80 cell extracts (control or depleted with 2 different shRNAs). (c) immunofluorostaining against cJun (rhodamine, DAPI for nuclei) on MSC80 cells (control or depleted with 2 different shRNAs). (d) RT-qPCR and (e) WB of 4-OH TM-treated SC primary culture extracts from $PLP^{+/+}KIAA1199^{loxp/loxp}$ (WT) and $PLP^{CreERT/+}$ $KIAA1199^{loxp/loxp}$ (iKO) mice. (f) immunofluorostaining against cJun (rhodamine, DAPI for nuclei) on 4-OH TM-treated SC primary cultures from WT and iKO mice. Data are expressed as mean ± SEM. Statistics: (a) one-way ANOVA followed by Dunnett's post-hoc analysis, $n = 3$–4 in all groups for each qPCR; (d) unpaired Student's t test, $n = 3$ in both groups; * $p < 0.05$, ** $p < 0.01$, *** $p < 0.001$. Scale bars: (c and f) 50 μm

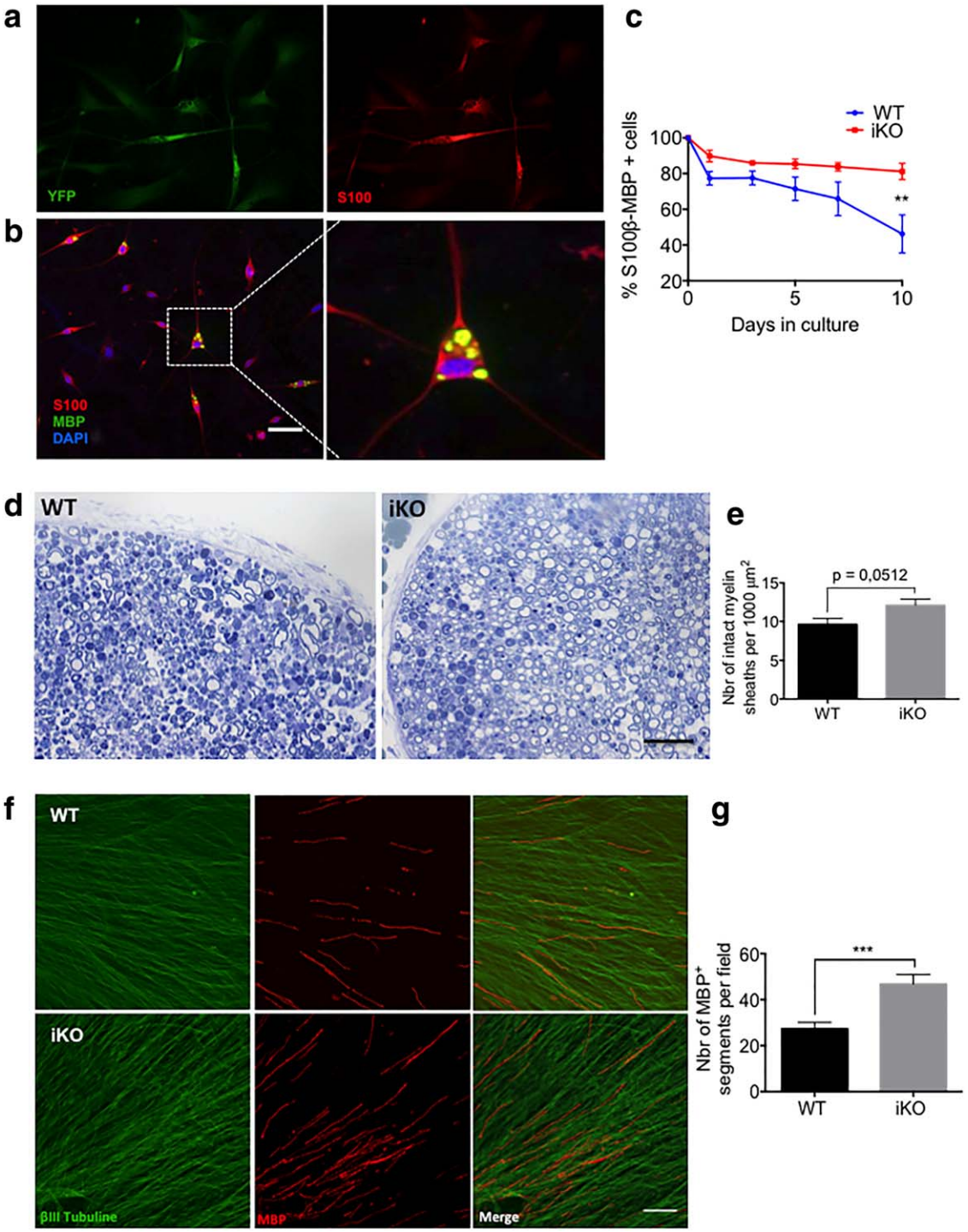

FIGURE 3 Role of KIAA1199 in SC myelin breakdown and myelination *ex vivo*. (a) Primary SCs isolated from sciatic and trigeminal nerves of P9 $PLP^{CreERT/+}$ $KIAA1199^{loxp/loxp}$ (iKO) mice, immunostained for YFP and S100, to illustrate the efficacy of the cre-recombination at P9. (b) Illustration of the immunofluorostaining against S100 (rhodamine) and MBP (FITC) on primary SCs isolated from sciatic and trigeminal nerves of P9 mice (either $PLP^{+/+}KIAA1199^{loxp/loxp}$ (WT) either $PLP^{CreERT/+}$ $KIAA1199^{loxp/loxp}$ (iKO), after 10 days in culture supplemented with 4-OH TM for the first 2 days. (c) Percentages of primary SCs (S100 positive) from WT and iKO mice containing MBP (as illustrated in the enlarged frame) at different time points after plating. (d) Toluidine blue-stained semi-thin sections showing relative preservation of intact myelin sheaths in WT and iKO tibial nerve segments after 4 days in pro-degeneration medium supplemented with 4-OH TM for the first 2 days. (e) Myelin sheath counts in tibial nerves after 4 days in pro-degeneration medium. (f) immunofluorostaining against MBP (rhodamine) and βIII Tubulin (FITC) on 4-OH TM-treated DRG explants from WT and iKO mice. (g) Quantification of the number of MBP-positive segments in 4-OH TM-treated DRG explants from WT and iKO mice. Data are expressed as mean ± SEM. Statistics: (c) two-way ANOVA followed by Sidak's post-hoc analysis, $n = 3$ in both groups; (e) unpaired Student's t test, $n = 4$ in both groups; (g) unpaired Student's *t* test, $n = 13$ for WT and 9 for iKO; ** $p < 0.01$, *** $p < 0.001$. Scale bars: (b) 50 µm, (d) 20 µm, (f) 100 µm

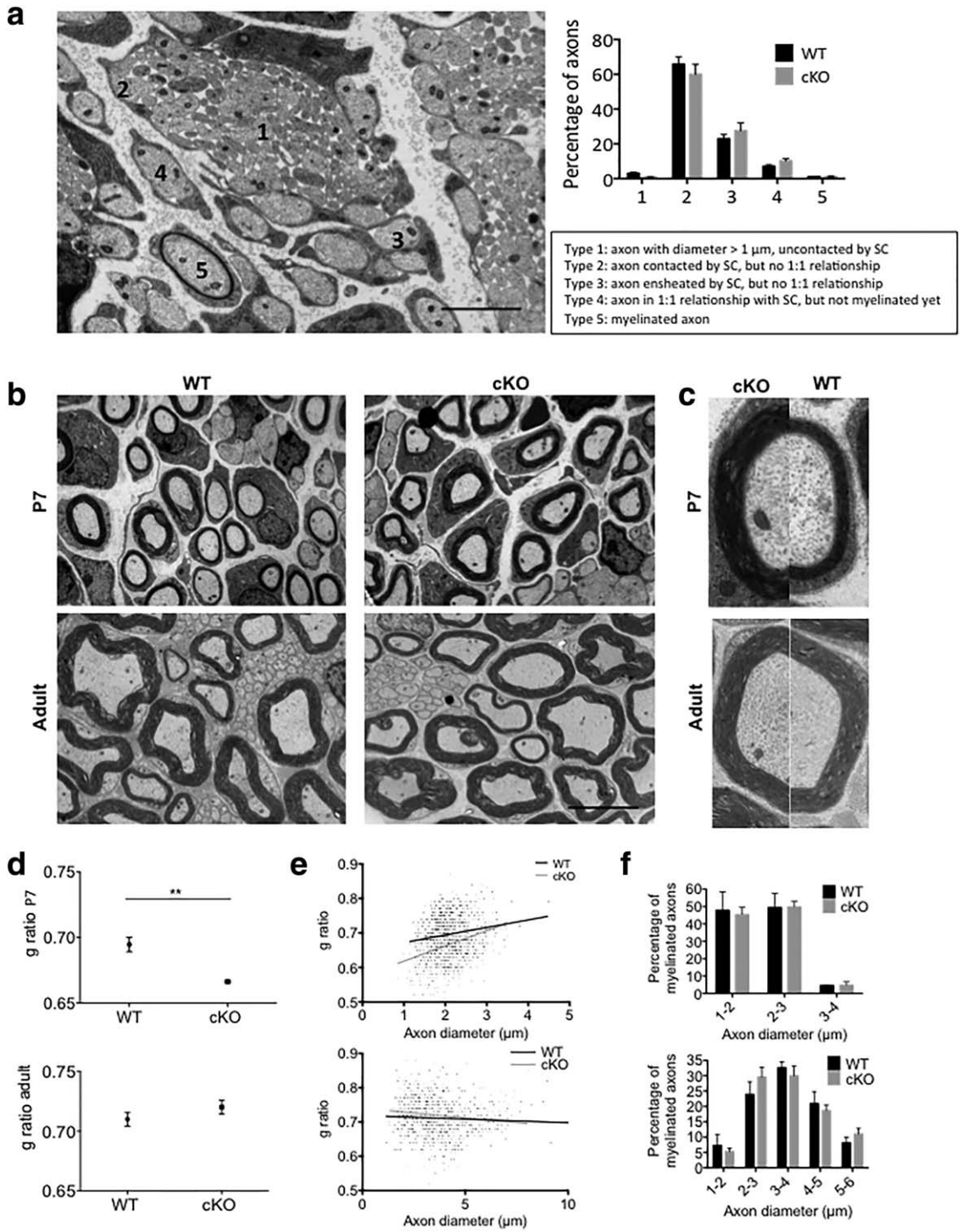

FIGURE 4 Role of KIAA1199 in radial sorting, in post-natal and adult myelination. Electron micrograph of a transversal section (75 nm) from WT and cKO P0-P1 (a), P7 and adult (b-c) tibial nerves. (a) Percentage of axons undergoing axonal sorting in P0-P1 WT and cKO tibial nerves. (d) Mean g ratios from P7 and adult WT and cKO nerves. $N = 3$ mice/group, adult: 379 axons for WT and 396 axons for cKO; P7: 506 axons for WT and 621 axons for cKO. (e) Scatter plot of *g* ratio versus axon diameter for P7 and adult WT and cKO nerves. (f) Percentage of myelinated axons per axonal caliber in P7 and adult sciatic nerves of WT and cKO mice. Data are expressed as mean ± SEM. Statistics: (d) unpaired Student's *t* test, $n = 3$ in both groups; ** $p < 0.01$. Scale bar: 5 µm

demonstrated that PLP$^{CreERT/+}$ KIAA1199$^{loxp/loxp}$ SCs form significantly more MBP-positive segments compared to WT cells, respectively, 46.83 ± 4.10 and 27.33 ± 2.84 (Figure 3g), indicating that *KIAA1199* inactivation in dedifferentiated SCs facilitates myelination. Collectively, our data suggest that KIAA1199 promotes SCs dedifferentiation and acts as a negative regulator of myelination.

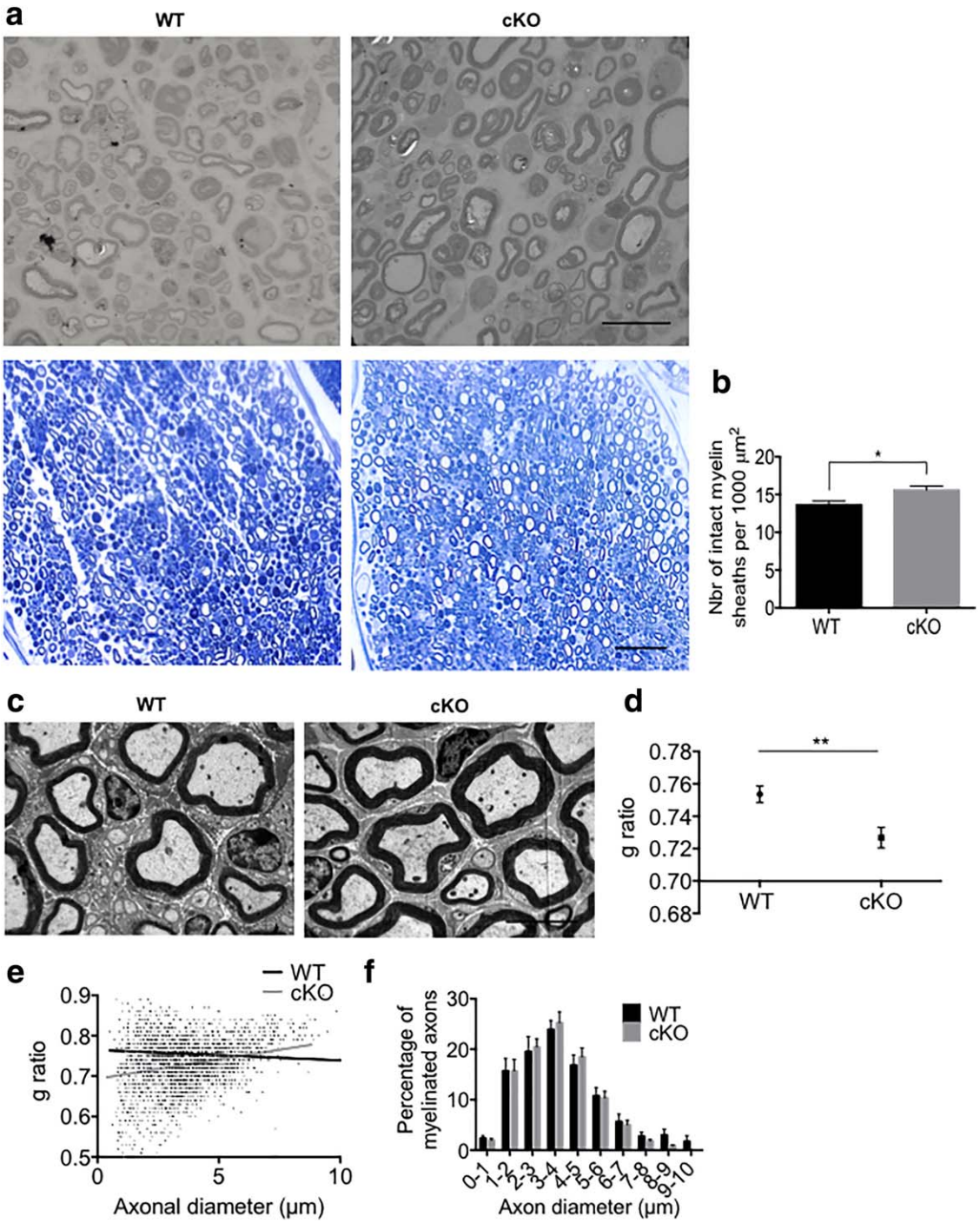

FIGURE 5 Role of KIAA1199 in SC myelin clearance, remyelination, and functional recovery after injury. (a) Electron micrographs (75-nm thickness) and semi-thin toluidine blue-stained sections (1-µm thickness) showing relative preservation of intact myelin sheaths in WT and cKO nerves, 3 days post-axotomy, 3-mm distal from axotomy site (transversal sections). (b) Counts of intact myelin sheaths in tibial nerves from WT and cKO mice 3 days after cut. (c) Electron micrographs of WT and cKO nerves, 2 months post-crush, 3-mm distal from the crush site (transversal sections, 75-nm thickness). (d) Average g ratios from WT and cKO adult nerves 2 months post-crush. (e) Scatter plot of *g* ratio versus axon diameter for WT and cKO nerves 2 months post-crush. $N = 1194$ axons, 7 mice (WT) and 1448 axons, 9 mice (cKO). (f) Percentages of myelinated fibers versus axon diameter in WT and cKO nerves 2 months post-crush. Data are expressed as mean ± SEM. Statistics: (b) unpaired Student's *t* test, $n = 4$ in both groups; (d) unpaired Student's *t* test, $n = 7$ for WT and 9 for cKO. * $p < 0.05$, ** $p < 0.01$, Scale bars: (a) 20 µm and 100 µm, (c) 5 µm [Color figure can be viewed at wileyonlinelibrary.com]

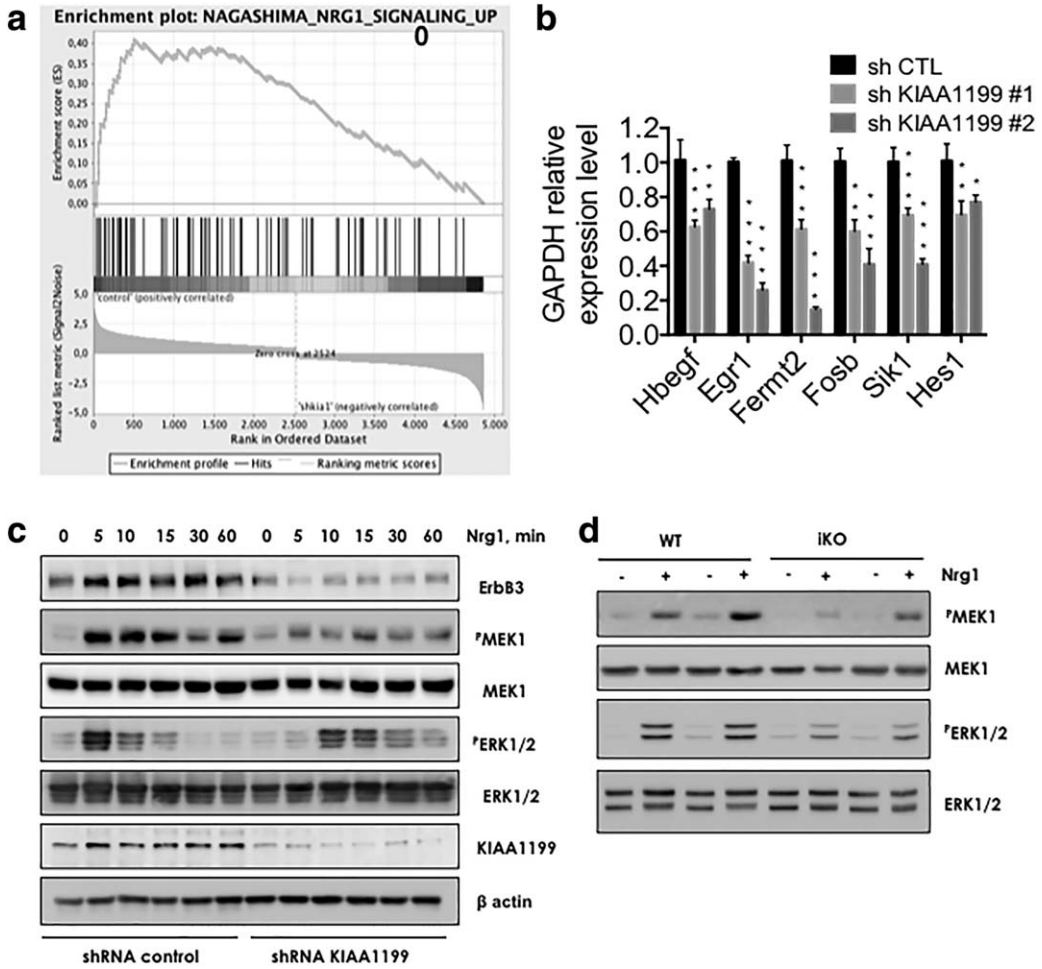

FIGURE 6 Role of KIAA1199 in Nrg1-signalling and Nrg1-induced MEK1/ERK1/2 phosphorylation. (a) Gene Set Enrichment Analysis (GSEA) enrichment plots of the Nrg1-regulated genes indicates significant positive enrichment in control compared to KIAA1199-depleted MSC80 cells (Normalized Enrichment Score = 2,297 and p value < 0.001, $n = 5$/group). (b) Nrg1-target gene RT-qPCR of MSC80 cell extracts (control or depleted with 2 different shRNAs). (c) Control or KIAA1199-depleted MSC80 cells were serum starved and were stimulated with Nrg1 (10 ng/mL) for the indicated periods of time. WB analysis on the resulting cell extracts reveals a decreased expression of ErbB3 and a delay/decrease in the phosphorylation of MEK and ERK. (d) Primary SCs from $PLP^{+/+}KIAA1199^{loxp/loxp}$ (WT) and $PLP^{CreERT/+}$ $KIAA1199^{loxp/loxp}$ (iKO) mice, treated for 2 days with 4-OH TM, serum starved and stimulated with Nrg1 (10 ng/mL) for 10 min. WB on the resulting cell extracts revealed a decreased phosphorylation of MEK and ERK when KIAA1199 is decreased. Data are expressed as mean ± SEM. Statistics: (b) one-way ANOVA followed by Dunnett's post-hoc analysis, $n = 3$ in all groups for each qPCR; * $p < 0.05$, ** $p < 0.01$, *** $p < 0.001$

3.4 | KIAA1199 deficiency in mice transiently accelerates post-natal myelination without affecting adult myelin

In order to test whether KIAA1199 suppression in mice would affect developmental myelination (radial sorting and post-natal myelination), we crossed the KIAA1199 floxed mouse with another transgenic mouse in which the Cre recombinase expression is under the control of the desert hedgehog (DHH) promoter (= cKO mouse). EM performed on transverse sciatic nerve sections from P0-P1 WT and cKO mice did not reveal any difference in the radial sorting of the SCs (Figure 4a). However, at P7, the mean g ratio calculated for over 500 fibers from both WT and cKO nerves was significantly lower in cKO mice (g ratio = 0.666 ± 0.0007) compared to WT mice (g ratio = 0.695 ± 0.005), revealing an acceleration of myelination in the absence of KIAA1199 in SCs (Figure 4b-f). In adult mice, no obvious abnormalities were noticed in the overall nerve architecture of cKO animals, as assessed by morphological examinations (Figure 4b–f). The myelin sheath thickness was also evaluated by EM analysis and no statistical difference was observed in the mean g ratios of WT (g ratio = 0.71 ± 0.01) and cKO (g ratio = 0.72 ± 0.01) animals (Figure 4d). The numbers of myelinated and unmyelinated fibers was also similar (data not shown). Therefore, KIAA1199 is dispensable for myelination but its absence transiently accelerates myelination. KIAA1199 could thus be considered as a novel negative regulator of myelination.

3.5 | KIAA1199 is required for SC myelin breakdown after injury and its inactivation facilitates remyelination

Because KIAA1199 promotes SC dedifferentiation and myelin clearance, two essential events taking place after injury, we investigated

KIAA1199 functions following nerve injury. We performed nerve axotomy in which the proximal stump was pulled aside to prevent regeneration and favor SC dedifferentiation. Three days later, EM analysis of myelin sheath fragmentation 3 mm from the injured site revealed a significant higher number of intact myelin sheaths in the cKO nerves ($15.60 \pm 0.51/1000\ \mu m^2$) compared to WT ($13.65 \pm 0.50/1000\ \mu m^2$), indicating a role for KIAA1199 in myelin degradation after injury (Figure 5a and b).

To investigate whether *KIAA1199* inactivation in SCs would impact remyelination and functional recovery following injury, we crushed the sciatic nerves of WT and cKO animals in order to allow axon regeneration. The myelin sheath thickness was assessed on electron micrographs of WT and cKO nerves 2 months after crush (Figure 5c). We found a smaller mean *g* ratio in cKO nerves (0.727 ± 0.006) compared to WT (0.754 ± 0.005), pointing out a significant increased myelin thickness when KIAA1199 is decreased (Figure 5d). The scatter plot of *g* ratio versus axon diameter indicated that the myelin thickness is particularly increased for the smallest axons and that the overall distribution of myelinated fibers is unaffected when KIAA1199 is decreased (Figure 5e and f, respectively). To determine the possible function of KIAA1199 in sensory and motor functional recovery, behavioral tests were performed on WT and cKO animals. Measurements of sciatic functional index and Von Frey threshold and observations of the toe-spreading reflex revealed no differences in the recovery between WT and cKO animals at any of the time-points tested (Supporting Information, Figure S1c-e). Taken together, our data indicate that the absence of KIAA1199 not only delays SC dedifferentiation after nerve injury, but also increases remyelination. Again, KIAA1199 could thus be considered as a negative regulator of myelination.

3.6 | KIAA1199 is required for Nrg1-signalling and MEK1/ERK1/2 phosphorylation

To gain more information about molecular mechanisms by which KIAA1199 acts on SC dedifferentiation, we profiled the transcriptome of control and KIAA1199-depleted MSC80 cells to identify pathways specifically deregulated upon KIAA1199 depletion. Total RNAs were extracted and subjected to high throughput RNA sequencing. Interestingly, a gene set enrichment analysis (GSEA) highlighted a significant and specific Nrg1-dependent signature that was decreased in KIA1199-depleted cells (Figure 6a). Real-Time PCR analysis confirmed that selected Nrg1 target mRNAs (Topilko et al., 1997; Mercier, Turque, & Schumacher, 2001; Amin, Tuck, & Stern, 2005; Gao, Daugherty, & Tourtellotte, 2007; Nagashima et al., 2007; Woodhoo et al., 2009; Ji et al., 2012; Adams et al., 2017) were down regulated in KIAA1199-depleted MSC80 cells (Figure 6b).

Given the fact that Nrg1 has been suggested as the potential signal driving SC dedifferentiation through Raf/MEK1/ERK1/2 signalling (Napoli et al., 2012), we analyzed whether KIAA1199 deficiency would impair this pathway. To test this, we serum-starved and stimulated or not control or KIAA1199-depleted MSC80 cells with Nrg1 (10 ng/mL) for different periods of time. WB analysis demonstrated a decreased expression of ErbB3 and a delay in the phosphorylation of both MEK1 and ERK1/2 (Figure 6c). We also cultured primary SCs from WT and iKO mice and treated them for 2 days with 4-OH TM to induce recombination, then serum starved and stimulated with Nrg1 for 10 minutes. The WB analyses again revealed a decreased phosphorylation of both MEK1 and ERK1/2 when KIAA1199 is decreased (Figure 6d). Therefore, KIAA1199 promotes Ngr1-dependent MEK1 and ERK1/2 activation in SCs.

4 | DISCUSSION

Nerve regeneration involves complex multicellular and molecular events in which SCs play a role of orchestrator (Cattin & Lloyd, 2016). The signal that induces this pro-healing response remains unknown but originates from damaged nerves and instructs SCs to reprogram into specialized repair cells, named "transdifferentiated" cells (Arthur-Farraj et al., 2012). The remarkable ability of SCs to dedifferentiate has been extensively studied but the molecular mechanisms that modulate their plasticity only start to be elucidated (Boerboom, Dion, Chariot, & Franzen, 2017). Whereas the role of cJun or Notch as key players for SC reprogramming is well established, the function of some pathways including Nrg1/ErbB and MEK1/ERK1/2 signalling remains unclear. Indeed, these pathways have been demonstrated to regulate both SC differentiation and plasticity depending on their quantitative and temporal activation. In one hand, the ectopic activation of Raf in cultured differentiated SCs drives their dedifferentiation even in co-cultures with DRG-neurons (Harrisingh et al., 2004). More recently, Napoli et al. (2012) revealed that a Tamoxifen-inducible Raf transgene in SCs is sufficient to provoke the down-regulation of myelin proteins and the expression of dedifferentiation markers *in vivo*, even in the absence of axonal damage. On the other hand, different studies showed that ERK1/2 activation is actually a pro-myelinating signal and that its inhibition blocks SC differentiation and myelination *in vivo* (Grossmann et al., 2009; He et al., 2010; Newbern et al., 2011). The reconciling hypothesis could be that different levels of ERK1/2 activation would define the state of SC differentiation. Low or basal ERK1/2 activity would induce SC myelination while high ERK1/2 levels would drive their dedifferentiation (Newbern & Snider, 2012). Consistently, Syed et al. (2010) demonstrated that a robust activation of ErbB2/3 via high concentration of Nrg1 provokes demyelination and increased cJun levels in SC cultures. Thus, the identification of potential regulators of MEK1/ERK1/2 signalling could help to decipher the context-specific aspects driving the effects of this pathway on SC plasticity. In this study, we investigated the potential role of KIAA1199, a protein that promotes ErbB and MEK1/ERK1/2 signalling in cancer cells, in SC biology. Mechanistically, we confirmed that KIAA1199 is necessary for Nrg1-induced MEK1/ERK1/2 phosphorylation, both in MSC80 cells and primary SCs, reinforcing our hypothesis that KIAA199 could play a role in SC myelination and dedifferentiation.

Our *in vitro* and *ex vivo* results indicate that KIAA1199 is necessary to induce and maintain SC dedifferentiation. Indeed, when KIAA1199 is depleted in MSC80 cells or suddenly inactivated in primary cultures, the dedifferentiated SCs tend to differentiate, as assessed by the increase of Krox20 mRNA levels and the decreased expression of

dedifferentiation markers such as cJun, Notch or DDIT4. In our *ex vivo* experiments using the inducible mouse model in which long-term compensatory mechanisms are prevented, we show that myelin clearance and breakdown are decreased when *KIAA1199* is inactivated in SCs. Consistently, the sudden inactivation of *KIAA1199* by the addition of 4-OH TM in dedifferentiated SCs facilitates myelination in DRG explants. The suppression of molecular components playing a role in SC dedifferentiation is known to increase myelination. For example, the deletion of cJun in cultured SCs strikingly accelerates Krox20-induced expression of MBP or MPZ (Parkinson et al., 2008). Moreover, the inactivation of Notch signalling *in vivo* leads to premature myelin formation and the loss of DDIT4 expression both *in vitro* and *in vivo* results in sustained hypermyelination (Woodhoo et al., 2009; Noseda et al., 2013).

Consistently with a role of KIAA1199 in Nrg1-dependent ErbB and MEK1/ERK1/2 signallings, we expected some defects in SC myelination in the absence of KIAA1199 in mice. Indeed, several studies showed that those pathways control both the development of SCs and the myelination program (Britsch et al., 1998; Woldeyesus et al., 1999; Garratt, Britsch, & Birchmeier, 2000; Birchmeier & Nave, 2008; Grossmann et al., 2009; Newbern & Birchmeier, 2010; Newbern et al., 2011). Using a mouse model in which KIAA1199 is inactivated in SCs at E12, we indeed show a transient acceleration of myelination at P7, without any defects in the radial sorting at P0-P1. Surprisingly, the analyses of this mutant mouse at adult stage did not show any detectable defects in myelin. This could potentially be attributed to residual KIAA1199 levels in the knockout mouse but also to the complexity of *in vivo* systems in which compensatory mechanisms and functional overlap may hide the detection of a phenotype. Since KIAA1199 participates in the modulation of Nrg1-induced MEK1/ERK1/2 activation, its residual levels in mutant mice could be sufficient for normal SC development. Finally, in situations in which MEK1/ERK1/2 signalling is highly activated (i.e., after injury), the expression of KIAA1199 in the conditional knockout mice may be diminished enough to highlight its function.

ERK1/2 signalling is highly activated following injury and plays a key role in initiating demyelination triggered by nerve damage and other pathological conditions (Sheu, Kulhanek, & Eckenstein, 2000; Harrisingh et al., 2004; Napoli et al., 2012; Fledrich et al., 2014). Nrg1 has been proposed to be the signal that activates MEK1/ERK1/2-induced dedifferentiation and it has been shown that the direct binding of Mycobacterium leprae on ErbB2 on SCs results in the activation of ERK1/2 signalling and demyelination (Tapinos et al., 2006; Napoli et al., 2012). Also, the Nrg1/ErbB system is highly regulated during peripheral nerve degeneration, which further supports its role in SC plasticity (Carroll, Miller, Frohnert, Kim, & Corbett, 1997; Kwon et al., 1997; Napoli et al., 2012; Ronchi et al., 2016). Guertin, Zhang, Mak, Alberta, and Kim (2005) showed that ErbB2 is activated in SCs after sciatic nerve injury and that its transient activation is sufficient to induce demyelination in compartmentalized cell culture chambers. They also showed that the treatment of rats with an ErbB2 inhibitor leads to a reduction of demyelination after nerve transection. Furthermore, *in vitro* experiments imitating nerve lesions revealed that Nrg1 treatment is beneficial for SC response to damage (Mahanthappa, Anton, & Matthew, 1996; Li, Wigley, & Hall, 1998). However, Atanasoski et al. (2006) revealed contradictory results. They showed that the lack of ErbB2 in adult SCs does not disturb their proliferation and survival after nerve injury, despite reduced levels of phosphorylated MAPK. Our examinations on the mutant mice after nerve injury provide evidence that KIAA1199 promotes myelin breakdown and SC dedifferentiation. Moreover, in consistency with the fact that decreased KIAA1199 expression in dedifferentiated SCs tend to boost their differentiation, we observed a small but significant increase of the myelin sheath thickness following injury in the mutant nerves. However, the functional effect of the decreased expression of KIAA1199 on SC plasticity is quite mild, as it did not disturb the overall recovery after injury. Let's note however that some neurophysiological parameters like nerve conduction velocity remain to be investigated.

In agreement with the literature, our results strongly suggest that KIAA1199 acts in the Nrg1-induced MEK1/ERK1/2 signalling pathway to modulate SC dedifferentiation. Our data also support the findings that Nrg1/ErbB and MEK1/ERK1/2 signallings are involved in SC plasticity, which may define new therapies that specifically target SC dedifferentiation and regenerative potential to enhance repair. However, this approach should be cautioned since enhanced activation of Nrg1/ErbB and MEK1/ERK1/2 signalling can lead to the development of nerve tumours (Frohnert, Stonecypher, & Carroll, 2003; Fallon, Havlioglu, Hamilton, Cheng, & Carroll, 2004; Harrisingh et al., 2004; Tapinos et al., 2006). Consistently, KIAA1199 is increased in multiple solid tumours and represents a promising target to interfere with ErbB signalling in cancer (Matsuzaki et al., 2009; Kuscu et al., 2012; Tiwari et al., 2013; Shostak et al., 2014). While this study identified KIAA1199 as a new modulator of Nrg1/MEK1/ERK1/2-induced SC plasticity, further mechanistical studies are required to elucidate the exact molecular functions of KIAA1199 in SC biology.

ACKNOWLEDGMENT

This work was supported by Grants from the Belgian National Funds for Scientific Research (FRS-FNRS), the Fonds Léon Fredericq from the University of Liege, the « Fondation Charcot » from Belgium, and the «Association Belge contre les Maladies Neuro-Musculaires, ABMM ». We are also grateful to the GIGA imaging, genomics and viral vector facilities (GIGA, University of Liege). A.C. is a Research Director at the FNRS and is supported by grants from the WELBIO and the Belgian Foundation against cancer.

REFERENCES

Abe, S., Usami, S., & Nakamura, Y.. (2003). Mutations in the gene encoding KIAA1199 protein, an inner-ear protein expressed in Deiters' cells and the fibrocytes, as the cause of nonsyndromic hearing loss. *Journal of Human Genetics*, *48*, 564–570.

Adams, K. W., Kletsov, S., Lamm, R. J., Elman, J. S., Mullenbrock, S., & Cooper, G. M. (2017). Role for Egr1 in the transcriptional program associated with neuronal differentiation of PC12 cells. *PLoS One*, *12*, e0170076-

Amin, D. N., Tuck, D., & Stern, D. F. (2005). Neuregulin-regulated gene expression in mammary carcinoma cells. *Experimental Cell Research*, *309*, 12–23.

Arthur-Farraj, P. J., Latouche, M., Wilton, D. K., Quintes, S., Chabrol, E., Banerjee, A., Woodhoo, A., Jenkins, B., Rahman, M., Turmaine, M., Wicher, G. K., Mitter, R., Greensmith, L., Behrens, A., Raivich, G., Mirsky, R., & Jessen, K. R. (2012). c-Jun reprograms Schwann cells of injured nerves to generate a repair cell essential for regeneration. *Neuron*, *75*, 633–647.

Atanasoski, S., Scherer, S. S., Sirkowski, E., Leone, D., Garratt, A. N., Birchmeier, C., & Suter, U. (2006). ErbB2 signalling in Schwann cells is mostly dispensable for maintenance of myelinated peripheral nerves and proliferation of adult Schwann cells after injury. *Journal of Neuroscience*, *26*, 2124–2131.

Birchmeier, C., & Nave, K.-A. (2008). Neuregulin-1, a key axonal signal that drives Schwann cell growth and differentiation. *Glia*, *56*, 1491–1497.

Boerboom, A., Dion, V., Chariot, A., & Franzen, R. (2017). Molecular mechanisms involved in Schwann cell plasticity. *Frontiers in Molecular Neuroscience*, *10*, 38.

Britsch, S., Li, L., Kirchhoff, S., Theuring, F., Brinkmann, V., Birchmeier, C., & Riethmacher, D. (1998). The ErbB2 and ErbB3 receptors and their ligand, neuregulin-1, are essential for development of the sympathetic nervous system. *Genes & Development*, *12*, 1825–1836.

Carroll, S. L., Miller, M. L., Frohnert, P. W., Kim, S. S., & Corbett, J. A. (1997). Expression of neuregulins and their putative receptors, ErbB2 and ErbB3, is induced during Wallerian degeneration. *Journal of Neuroscience*, *17*, 1642–1659.

Cattin, A.-L., & Lloyd, A. C. (2016). The multicellular complexity of peripheral nerve regeneration. *Current Opinion in Neurobiology*, *39*, 38–46.

Chaballe, L., Close, P., Sempels, M., Delstanche, S., Fanielle, J., Moons, L., Carmeliet, P., Schoenen, J., Chariot, A., & Franzen, R. (2011). Involvement of placental growth factor in Wallerian degeneration. *Glia*, *59*, 379–396.

Creppe, C., Malinouskaya, L., Volvert, M.-L., Gillard, M., Close, P., Malaise, O., Laguesse, S., Cornez, I., Rahmouni, S., & Ormenese, S. (2009). Elongator controls the migration and differentiation of cortical neurons through acetylation of α-tubulin. *Cell*, *136*, 551–564.

Evensen, N. A., Kuscu, C., Nguyen, H.-L., Zarrabi, K., Dufour, A., Kadam, P., Hu, Y., Pulkoski-Gross, A., Bahou, W. F., & Zucker, S. (2013). Unraveling the role of KIAA1199, a novel endoplasmic reticulum protein, in cancer cell migration. *Journal of the National Cancer Institute*, *105*, 1402–1416.

Fallon, K. B., Havlioglu, N., Hamilton, L. H., Cheng, T. P. H., & Carroll, S. L. (2004). Constitutive activation of the neuregulin-1/erbB signaling pathway promotes the proliferation of a human peripheral neuroepithelioma cell line. *Journal of Neuro-Oncology*, *66*, 273–284.

Fledrich, R., Stassart, R. M., Klink, A., Rasch, L. M., Prukop, T., Haag, L., Czesnik, D., Kungl, T., Abdelaal, T. A. M., Keric, N., Stadelmann, C., Bruck, W., Nave, K.-A., & Sereda, M. W. (2014). Soluble neuregulin-1 modulates disease pathogenesis in rodent models of Charcot-Marie-Tooth disease 1A. *Nature Medicine*, *20*, 1055–1061.

Frohnert, P. W., Stonecypher, M. S., & Carroll, S. L. (2003). Constitutive activation of the neuregulin-1/ErbB receptor signaling pathway is essential for the proliferation of a neoplastic Schwann cell line. *Glia*, *43*, 104–118.

Gao, X., Daugherty, R. L., & Tourtellotte, W. G. (2007). Regulation of low affinity neurotrophin receptor (p75NTR) by early growth response (Egr) transcriptional regulators. *Molecular and Cellular Neuroscience*, *36*, 501–514.

Garratt, A. N., Britsch, S., & Birchmeier, C. (2000). Neuregulin, a factor with many functions in the life of a Schwann cell. *Bioessays*, *22*, 987–996.

Grossmann, K. S., Wende, H., Paul, F. E., Cheret, C., Garratt, A. N., Zurborg, S., Feinberg, K., Besser, D., Schulz, H., Peles, E., Selbach, M., Birchmeier, W., & Birchmeier, C. (2009). The tyrosine phosphatase Shp2 (PTPN11) directs Neuregulin-1/ErbB signaling throughout Schwann cell development. *Proceedings of the National Academy of Sciences of the United States of America*, *106*, 16704–16709.

Guertin, A. D., Zhang, D. P., Mak, K. S., Alberta, J. A., & Kim, H. A. (2005). Microanatomy of axon/glial signaling during Wallerian degeneration. *Journal of Neuroscience*, *25*, 3478–3487.

Harrisingh, M. C., Perez-Nadales, E., Parkinson, D. B., Malcolm, D. S., Mudge, A. W., & Lloyd, A. C. (2004). The Ras/Raf/ERK signaling pathway drives Schwann cell dedifferentiation. *embo J*, *23*, 3061–3071.

He, Y., Kim, J. Y., Dupree, J., Tewari, A., Melendez-Vasquez, C., Svaren, J., & Casaccia, P. (2010). Yy1 as a molecular link between neuregulin and transcriptional modulation of peripheral myelination. *Nature Neuroscience*, *13*, 1472–1480.

Inserra, M. M., Bloch, D. A., & Terris, D. J. (1998). Functional indices for sciatic, peroneal, and posterior tibial nerve lesions in the mouse. *Microsurgery*, *18*, 119–124.

Jessen, K. R., & Mirsky, R. (2005). The origin and development of glial cells in peripheral nerves. *Nature Reviews Neuroscience*, *6*, 671–682.

Jessen, K. R., & Mirsky, R. (2016). The repair Schwann cell and its function in regenerating nerves. *The Journal of Physiology*, *594*, 3521–3531.

Ji, Y., Shen, M., Wang, X., Zhang, S., Yu, S., Chen, G., Gu, X., & Ding, F. (2012). Comparative proteomic analysis of primary Schwann cells and a spontaneously immortalized Schwann cell line RSC 96, a comprehensive overview with a focus on cell adhesion and migration related proteins. *Journal of Proteome Research*, *11*, 3186–3198.

Kim, H. A., Mindos, T., & Parkinson, D. B. (2013). Plastic fantastic, Schwann cells and repair of the peripheral nervous system. *Stem Cells Translational Medicine*, *2*, 553–557.

Kuscu, C., Evensen, N., Kim, D., Hu, Y.-J., Zucker, S., & Cao, J. (2012). Transcriptional and epigenetic regulation of KIAA1199 gene expression in human breast cancer. *PLoS One*, *7*, e44661-

Kwon, Y. K., Bhattacharyya, A., Alberta, J. A., Giannobile, W. V., Cheon, K., Stiles, C. D., & Pomeroy, S. L. (1997). Activation of ErbB2 during wallerian degeneration of sciatic nerve. *Journal of Neuroscience*, *17*, 8293–8299.

Li, H., Wigley, C., & Hall, S. M. (1998). Chronically denervated rat Schwann cells respond to GGF in vitro. *Glia*, *24*, 290–303.

Mahanthappa, N. K., Anton, E. S., & Matthew, W. D. (1996). Glial growth factor 2, a soluble neuregulin, directly increases Schwann cell motility and indirectly promotes neurite outgrowth. *Journal of Neuroscience*, *16*, 4673–4683.

Matsuzaki, S., Tanaka, F., Mimori, K., Tahara, K., Inoue, H., & Mori, M. (2009). Clinicopathologic significance of KIAA1199 overexpression in human gastric cancer. *Annals of Surgical Oncology*, *16*, 2042–2051.

Mercier, G., Turque, N., & Schumacher, M. (2001). Rapid effects of triiodothyronine on immediate-early gene expression in Schwann cells. *Glia*, *35*, 81–89.

Nagashima, T., Shimodaira, H., Ide, K., Nakakuki, T., Tani, Y., Takahashi, K., Yumoto, N., & Hatakeyama, M. (2007). Quantitative transcriptional control of ErbB receptor signaling undergoes graded to biphasic response for cell differentiation. *The Journal of Biological Chemistry*, *282*, 4045–4056.

Napoli, I., Noon, L. A., Ribeiro, S., Kerai, A. P., Parrinello, S., Rosenberg, L. H., Collins, M. J., Harrisingh, M. C., White, I. J., & Woodhoo, A. (2012). A central role for the ERK-signaling pathway in controlling Schwann cell plasticity and peripheral nerve regeneration in vivo. *Neuron*, *73*, 729–742.

Newbern, J., & Birchmeier, C. (2010). Nrg1/ErbB signaling networks in Schwann cell development and myelination. *Seminars in Cell and Developmental Biology*, *21*, 922–928.

Newbern, J. M., Li, X., Shoemaker, S. E., Zhou, J., Zhong, J., Wu, Y., Bonder, D., Hollenback, S., Coppola, G., Geschwind, D. H., Landreth, G. E., & Snider, W. D. (2011). Specific functions for ERK/MAPK signaling during PNS development. *Neuron*, *69*, 91–105.

Newbern, J. M., & Snider, W. D. (2012). Bers-ERK Schwann cells coordinate nerve regeneration. *Neuron*, *73*, 623–626.

Noseda, R., Belin, S., Piguet, F., Vaccari, I., Scarlino, S., Brambilla, P., Martinelli Boneschi, F., Feltri, M. L., Wrabetz, L., Quattrini, A., Feinstein, E., Huganir, R. L., & Bolino, A. (2013). DDIT4/REDD1/RTP801 is a novel negative regulator of Schwann cell myelination. *Journal of Neuroscience*, *33*, 15295–15305.

Parkinson, D. B., Bhaskaran, A., Arthur-Farraj, P., Noon, L. A., Woodhoo, A., Lloyd, A. C., Feltri, M. L., Wrabetz, L., Behrens, A., Mirsky, R., & Jessen, K. R. (2008). c-Jun is a negative regulator of myelination. *The Journal of Cell Biology*, *181*, 625–637.

Ronchi, G., Haastert-Talini, K., Fornasari, B. E., Perroteau, I., Geuna, S., & Gambarotta, G. (2016). The Neuregulin1/ErbB system is selectively regulated during peripheral nerve degeneration and regeneration. *European Journal of Neuroscience*, *43*, 351–364.

Sheu, J. Y., Kulhanek, D. J., & Eckenstein, F. P. (2000). Differential patterns of ERK and STAT3 phosphorylation after sciatic nerve transection in the rat. *Experimental Neurology*, *166*, 392–402.

Shostak, K., Zhang, X., Hubert, P., Göktuna, S. I., Jiang, Z., Klevernic, I., Hildebrand, J., Roncarati, P., Hennuy, B., Ladang, A., Somja, J., Gothot, A., Close, P., Delvenne, P., & Chariot, A. (2014). NF-κB-induced KIAA1199 promotes survival through EGFR signaling. *Nature Communications*, *5*, 5232-

Siconolfi, L. B., & Seeds, N. W. (2001). Mice lacking tPA, uPA, or plasminogen genes showed delayed functional recovery after sciatic nerve crush. *Journal of Neuroscience*, *21*, 4348–4355.

Syed, N., Reddy, K., Yang, D. P., Taveggia, C., Salzer, J. L., Maurel, P., & Kim, H. A. (2010). Soluble neuregulin-1 has bifunctional, concentration-dependent effects on Schwann cell myelination. *Journal of Neuroscience*, *30*, 6122–6131.

Tapinos, N., Ohnishi, M., & Rambukkana, A. (2006). ErbB2 receptor tyrosine kinase signaling mediates early demyelination induced by leprosy bacilli. *Nature Medicine*, *12*, 961–966.

Terashima, M., Fujita, Y., Togashi, Y., Sakai, K., De Velasco, M. A., Tomida, S., & Nishio, K. (2014). KIAA1199 interacts with glycogen phosphorylase kinase beta-subunit (PHKB) to promote glycogen breakdown and cancer cell survival. *Oncotarget*, *5*, 7040–7050.

Tiwari, A., Schneider, M., Fiorino, A., Haider, R., Okoniewski, M. J., Roschitzki, B., Uzozie, A., Menigatti, M., Jiricny, J., & Marra, G. (2013). Early insights into the function of KIAA1199, a markedly overexpressed protein in human colorectal tumors. *PLoS One*, *8*, e69473-

Topilko, P., Levi, G., Merlo, G., Mantero, S., Desmarquet, C., Mancardi, G., & Charnay, P. (1997). Differential regulation of the zinc finger genes Krox-20 and Krox-24 (Egr-1) suggests antagonistic roles in Schwann cells. *Journal of Neuroscience Research*, *50*, 702–712.

Vogelaar, C. F., Vrinten, D. H., Hoekman, M. F. M., Brakkee, J. H., Burbach, J. P. H., & Hamers, F. P. T. (2004). Sciatic nerve regeneration in mice and rats: recovery of sensory innervation is followed by a slowly retreating neuropathic pain-like syndrome. *Brain Research*, *1027*, 67–72.

Woldeyesus, M. T., Britsch, S., Riethmacher, D., Xu, L., Sonnenberg-Riethmacher, E., Abou-Rebyeh, F., Harvey, R., Caroni, P., & Birchmeier, C. (1999). Peripheral nervous system defects in erbB2 mutants following genetic rescue of heart development. *Genes & Development*, *13*, 2538–2548.

Woodhoo, A., Alonso, M. B. D., Droggiti, A., Turmaine, M., D'Antonio, M., Parkinson, D. B., Wilton, D. K., Al-Shawi, R., Simons, P., Shen, J., Guillemot, F., Radtke, F., Meijer, D., Feltri, M. L., Wrabetz, L., Mirsky, R., & Jessen, K. R. (2009). Notch controls embryonic Schwann cell differentiation, postnatal myelination and adult plasticity. *Nature Neuroscience*, *12*, 839–847.

Yoshida, H., Nagaoka, A., Kusaka-Kikushima, A., Tobiishi, M., Kawabata, K., Sayo, T., Sakai, S., Sugiyama, Y., Enomoto, H., & Okada, Y. (2013). KIAA1199, a deafness gene of unknown function, is a new hyaluronan binding protein involved in hyaluronan depolymerization. *Proceedings of the National Academy of Sciences United States of America*, *110*, 5612–5617.

Yoshino, Y., Ishisaka, M., Tsuruma, K., Shimazawa, M., Yoshida, H., Inoue, S., Shimoda, M., Okada, Y., & Hara, H. (2017). Distribution and function of hyaluronan binding protein involved in hyaluronan depolymerization (HYBID, KIAA1199) in the mouse central nervous system. *Neuroscience*, *347*, 1–10.

SUPPORTING INFORMATION

Additional Supporting Information may be found online in the supporting information tab for this article.

How to cite this article: Boerboom A, Reusch C, Pieltain A, Chariot A, Franzen R. KIAA1199: A novel regulator of MEK/ERK-induced Schwann cell dedifferentiation. *Glia*. 2017;65:1682–1696. https://doi.org/10.1002/glia.23188